JTTEE5 9:483-487

Plasma-Sprayed Nanostructured Al_2O_3/TiO_2 Powders and Coatings

B.H. Kear, Z. Kalman, R.K. Sadangi, G. Skandan, J. Colaizzi, and W.E. Mayo

(Submitted 8 October 1999; in revised form 21 April 2000)

Air plasma spray has been used to produce metastable oxide-ceramic powders and coatings, starting with commercially available $Al_2O_3/13TiO_2$ powder feed. The feed material undergoes rapid melting and homogenization in the high-temperature zone of the plasma jet. A metastable x-$Al_2O_3{\cdot}TiO_2$ phase is formed when the molten droplets are quenched on a chilled substrate. The metastable phase has a defect spinel structure and a nanocrystalline grain size. When heated, it decomposes into an equilibrium two-phase structure, consisting of α-Al_2O_3 and β-$Al_2O_3{\cdot}TiO_2$. Both types of ceramic materials have potential as hard, wear-resistant coatings.

Keywords air plasma spray, metastable phases, nanostructures, oxide coatings

1. Introduction

Recent research[1,2] on high-pressure sintering (HPS) of nanostructured oxide-ceramic materials has underscored the importance of using a starting powder that has a metastable structure. This is because a pressure-induced phase transition from metastable to stable state promotes consolidation at unusually low temperatures, typically <0.4 T_m. Moreover, the combination of high pressure and low temperature enables consolidation to be achieved without causing significant grain growth. In effect, high pressure causes prolific nucleation of the stable phase, while low temperature mitigates grain coarsening. Fully dense nanostructured ceramic materials are of interest because of their superior wear properties, relative to conventional ceramic materials.[3,4]

Because of the need for metastable powder feeds in the HPS process, we have been investigating alternative means for the production of test quantities of such powders. Three different approaches are currently being evaluated: (1) precipitation from a reactive solution at near ambient temperature, (2) rapid condensation from the vapor state, and (3) rapid solidification from the molten state.

In this paper, we report on preliminary work carried out on plasma melting and homogenization of a mixed $Al_2O_3/13TiO_2$ powder feed, followed by rapid solidification of the molten particles in cold water and on a chilled substrate. As will be shown, this work has demonstrated the ability to form a metastable $Al_2O_3{\cdot}TiO_2$ phase, with a nanocrystalline structure. Moreover, upon heat treatment, the metastable material transforms into the equilibrium two-phase structure, consisting of α-Al_2O_3 and β-$Al_2O_3{\cdot}TiO_2$. It is now realized that both types of structures have potential as hard, wear-resistant coating materials.

B.H. Kear, Z. Kalman, R.K. Sadangi, G. Skandan, J. Colaizzi, and **W.E. Mayo,** Center for Nanomaterials Research, Rutgers University, Piscataway, NJ 08854-8065. Contact e-mail: bkear@rci.rutgers.edu.

2. Experimental

Agglomerated powder feed of $Al_2O_3/13TiO_2$ (Metco 130, particle size −53 μm + 15 μm) was obtained from Sulzer Metco (Westbury, NY). An x-ray diffraction pattern of this powder showed that it was composed of a micron-scale mixture of α-Al_2O_3 (corundum) and TiO_2 (anatase) grains.

Plasma spraying was carried out at A&A Company Inc. (South Plainfield, NJ), using a Metco 3M gun. The powder was fed into a high-energy $N_2/10\%H_2$ plasma, with a protective argon shroud, and sprayed into cold water and onto a chilled substrate, located at 22 cm from the gun nozzle. The resulting powders, splats, and coatings were characterized by x-ray diffraction, using Cu K_α radiation (40 kV, 30 mA), and JADE (version 3.1, Materials Data Inc., Livermore, CA) for phase identification. Vickers hardness measurements were performed on polished sections using a microhardness tester (Leco Corp., St. Joseph, MI).

3. Results and Discussion

3.1 Effect of Cooling Rate

During the short residence time in the plasma jet, the feed particles were completely melted and homogenized. When the liquid droplets were water quenched, they solidified in one of two microstructural forms. Particles experiencing moderate cooling rates (~10^4 K/s) displayed a well-defined dendritic microstructure and exhibited some phase separation. However, particles experiencing somewhat higher cooling rates developed a cellular-dendritic microstructure. Both of these microstructures are shown in Fig. 1. When the cooling rate was exceptionally high, ~10^6 K/s, as in splat quenching on a metal chill plate, the microstructure was featureless. In other words, it appears that segregation-less (plane-front) solidification occurs only under the highest cooling rates characteristic of splat quenching.[5]

An x-ray diffraction pattern of the water-quenched powder (Fig. 2) shows that the dendritic structure is composed of an amorphous component, α-Al_2O_3, and metastable $Al_2O_3{\cdot}TiO_2$, which we call x phase. Our calculations indicate that the powder has approximately 50% amorphous content, 40% x phase, and

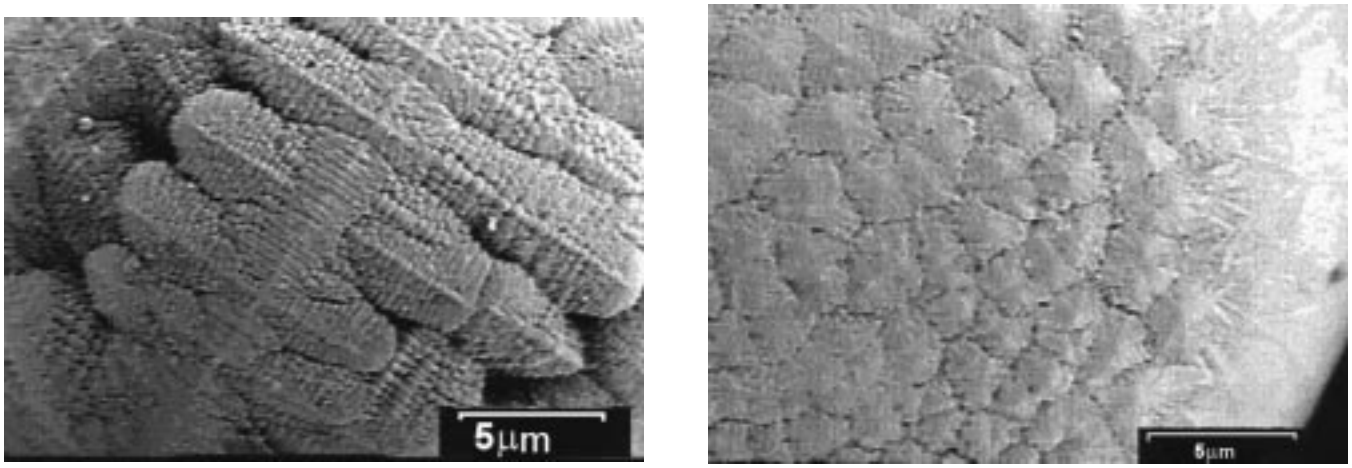

Fig. 1 Scanning electron micrographs of plasma-melted and water-quenched particles of Al_2O_3/TiO_2, showing dendritic (left) and cellular-dendritic (right) microstructures, depending on cooling rate

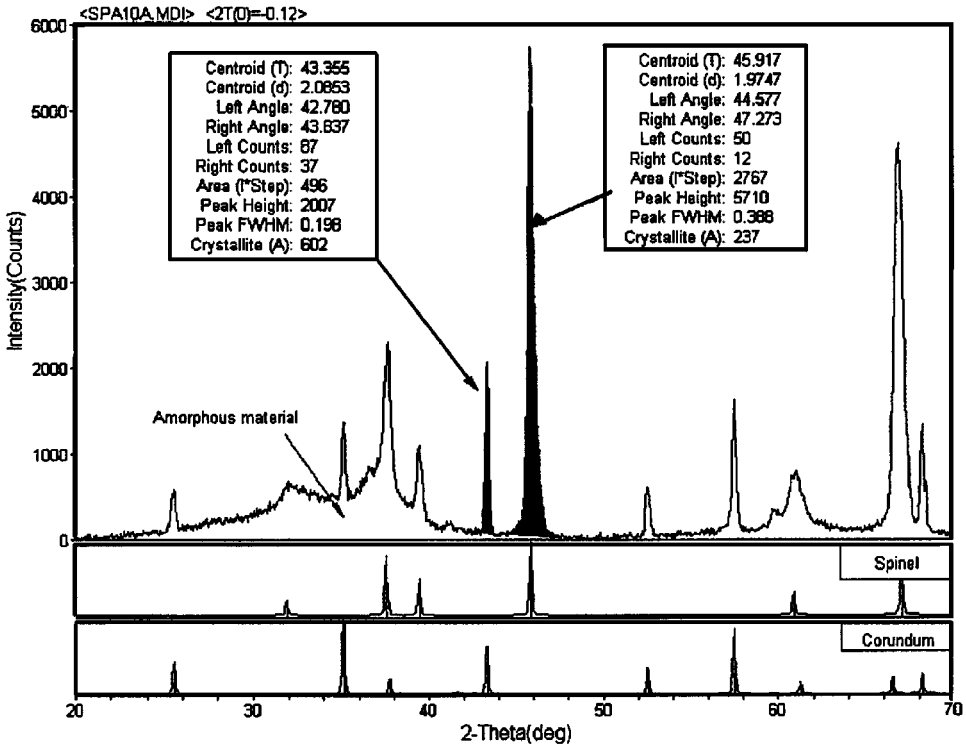

Fig. 2 X-ray diffraction pattern of Al_2O_3/TiO_2 powder, after plasma melting and water quenching. Shown for comparison are the reference diffraction patterns for the spinel and corundum (α-Al_2O_3) structures

10% α-Al_2O_3. The grain size of α-Al_2O_3 is between 60 and 80 nm, whereas that of the *x* phase is between 20 and 30 nm.[1] In contrast, the corresponding x-ray diffraction pattern of the splat-quenched powder (Fig. 3) shows evidence of a strong amorphous component plus *x* phase (20 to 30 nm grain size), but no α-Al_2O_3. The absence of α-Al_2O_3 phase is believed to be a consequence of the much higher average cooling rate experienced by splat-quenched material, relative to water-quenched material.

X-ray diffraction patterns similar to that of *x* phase have been reported in the literature. In particular, Zhou and Snyder[6] have given a detailed analysis of the diffraction patterns of chemically synthesized η-Al_2O_3 and γ-Al_2O_3 powders (Fig. 4). Both phases have a cubic structure—spinel with *Fd3m* space group. In this structure, the oxygen ions form a cubic close-packed sublattice, and the aluminum ions partially occupy both octahedral and tetrahedral sites. The broad peaks indicate a high degree of struc-

[1] Grain sizes were determined by applying crystallite size evaluation in the JADE program after $K_{\alpha 2}$ stripping and instrumental broadening correction.

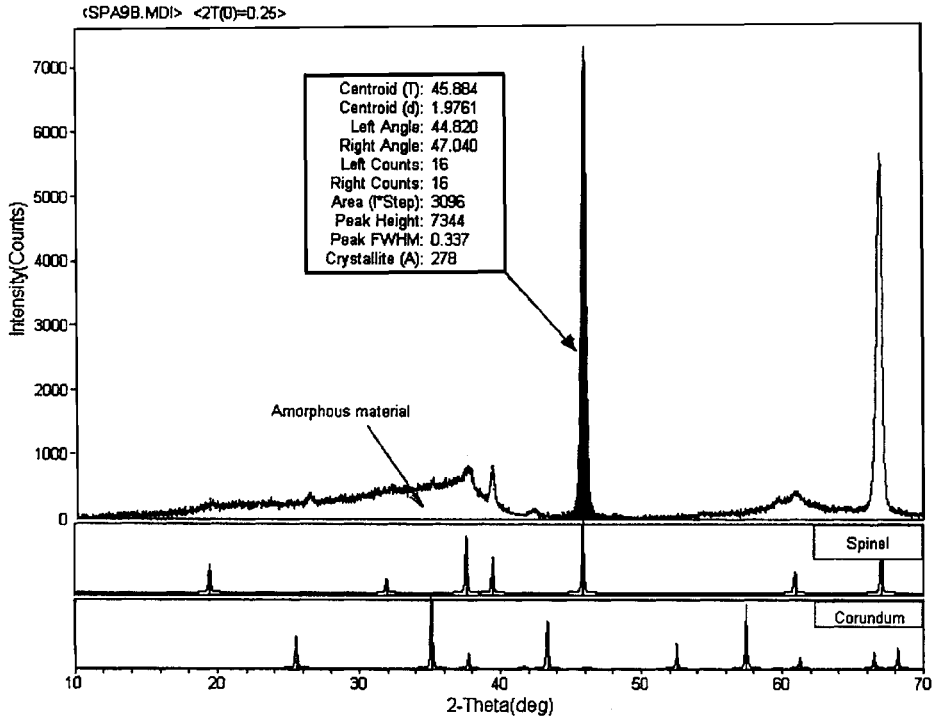

Fig. 3 X-ray diffraction pattern of Al_2O_3/powder, after plasma melting and splat quenching on a copper chill plate. Shown for comparison are the reference diffraction patterns for the spinel and corundum (α-Al_2O_3) structures

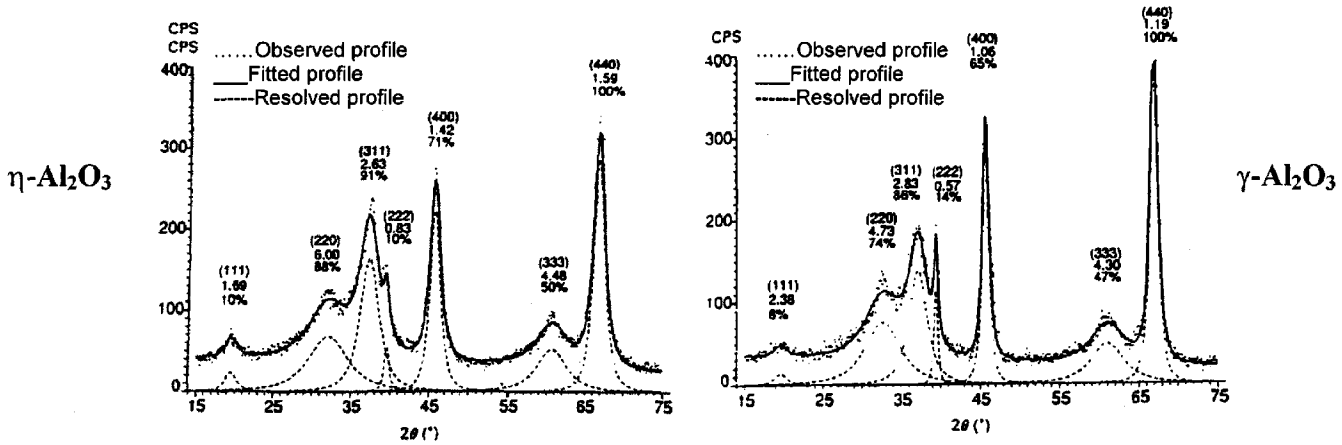

Fig. 4 X-ray diffraction patterns of chemically synthesized η-Al_2O_3 and γ-Al_2O_3 powders[6]

tural disorder, so that the material is more properly described as having a defect spinel structure. The sharp (222), (400), and (440) reflections are due to scattering from ordered domains of the oxygen sublattice.

In the present case (Fig. 3), the relative intensities of the (400) and (440) reflections are the opposite of that displayed by the η and γ phases. Computer simulations indicate that there is a preference for octahedral coordination of the cations, and that there is random occupancy of Ti on the Al lattice sites. It may be concluded, therefore, that the *x* phase is a metastable solid solution of Al_2O_3 and TiO_2. There are several features in the diffraction pattern that indicate a strongly disordered structure, which is far from equilibrium. First, note the presence of an amorphous phase, as indicated by the "hump" in the diffraction pattern at 35°. Also, the diffraction peaks are strong only for the spinel peaks at approximately 46 and 66.5°. All the other peaks for this phase have very low intensity.

An x-ray diffraction pattern of a typical plasma-sprayed coating showed similar features to that of the splat-quenched powder. This is to be expected, since a coating is formed by the superposition of splat-quenched particles. On the other hand, thick coatings produced by multiple passes showed some indications of α-Al_2O_3 formation, which probably reflects heating of the substrate, and hence lowering of the average quench rate.

Table 1 Summary of heat treatment data

Water-quenched powder				
Annealing temperature	**Qualitative composition (main phases)**		**Approximate quantitative compositions**	**Color**
RT	*x* phase	α-Alumina	10:1	Blue
800 °C	*x* phase	α-Alumina	7:1	Blue
1000 °C	*x* phase	α-Alumina unidentified phase(s)	9:2:?	Blue-gray
1200 °C	α-Alumina	*y* phase	9:2	Yellow-white
1400 °C	α-Alumina	β-Aluminum titanate *y* phase	20:3:1	White

x phase: cubic, $a_0 = 7.94$ A; $Al_2O_3 \cdot TiO_2$ cell dimensions close to those of γ-alumina (defect spinel structure)
y phase: tetragonal, $a_0 = 4.59$, $c_0 = 2.96$; $Al_2O_3 \cdot TiO_2$ cell dimensions close to that of $AlTiTaO_6$
β-$Al_2O_3 \cdot TiO_2$: orthorhombic, $a_0 = 3.56$, $b_0 = 9.44$, $c_0 = 9.65$

Table 2 Summary of heat treatment date

Splat-quenched coating				
Annealing temperature	**Qualitative composition (main phases)**		**Approximate quantitative compositions**	**Hardness (kg/mm², 1 kg load)**
RT	*x* phase	. . .	. . .	700
800 °C	*x* phase	. . .	. . .	720
1000 °C	α-Alumina	*x* phase or α-alumina unidentified phase(s)	3:1:?	850
1200 °C	α-Alumina	Ti_3O_5	100:1	940
1400 °C	α-Alumina	β-Aluminum titanate	4:1	990

x phase: cubic, $a_0 = 7.94$ A; $Al_2O_3 \cdot TiO_2$ cell dimensions close to those of γ-alumina (defect spinel structure)
Relative weight compositions were evaluated from the diffraction pattern, utilizing the I/Ic ratios published by the Joint Committee for Powder Diffraction Pattern, set 48

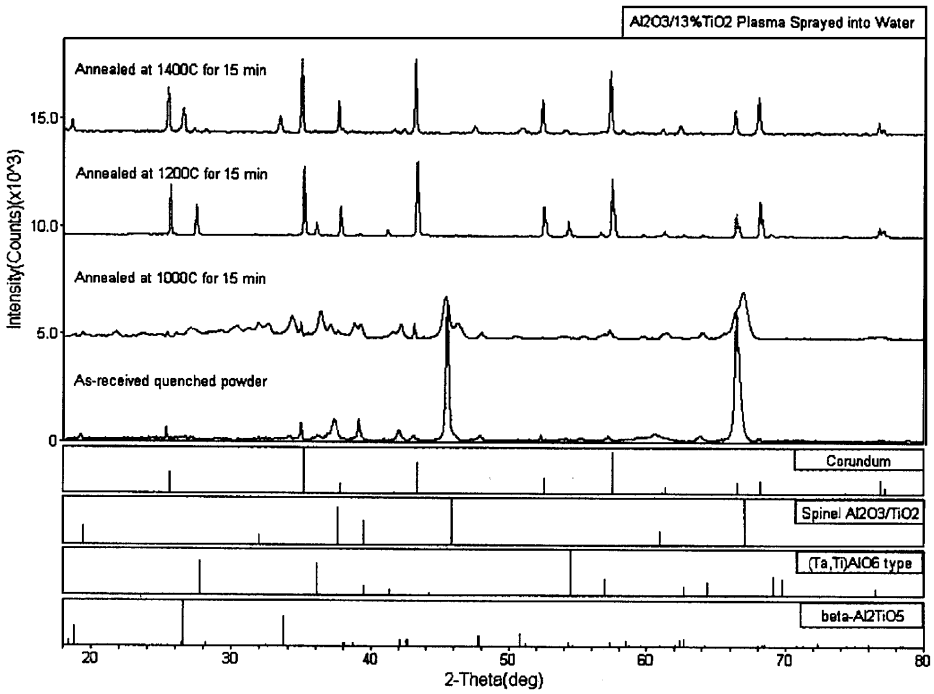

Fig. 5 X-ray diffraction patterns of water-quenched and heat-treated Al_2O_3/TiO_2 powder, showing decomposition reactions with increasing temperature

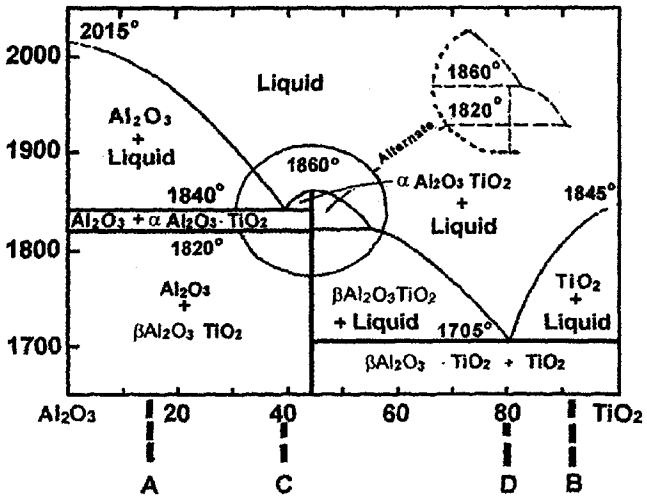

Fig. 6 Phase diagram for the Al_2O_3-TiO_2 system[7]

3.2 Effect of Heat Treatment

When water-quenched powder is heated at temperatures below 1200°C, a series of intermediate phases are formed (Table 1). At 1000 °C, the first such intermediate phase to appear has an unknown structure, with no known structural analogue. At 1200°C, a tetragonal phase appears, which is similar to the Al-$TaTiO_6$ crystal structure described in Powder Diffraction File (PDF) #32-0028. This phase is also metastable, and further decomposes at 1400 °C into the equilibrium two-phase structure, consisting of an approximately 1:1 mixture of β-Al_2O_3 and α-$Al_2O_3{\cdot}TiO_2$ (orthorhombic structure, PDF #41-0258). Thus, the final structure consists of primary α-Al_2O_3 (micrometer scale) and secondary α-Al_2O_3 that coprecipitates with the β-$Al_2O_3{\cdot}TiO_2$. Figure 5 illustrates these phase transitions *via* their respective x-ray diffraction patterns.

When splat-quenched material (powder or coating) is heated, thermal decomposition of the original *x* phase follows a somewhat different path (Table 2). The most notable change is the appearance of α-Al_2O_3 at 1000 °C as a major phase. Again, however, the equilibrium two-phase structure is established at 1400 °C. These phase transitions with increasing temperature are accompanied by a progressive increase in hardness, as indicated in Table 2. It is significant that the final structure at 1400 °C has a Vickers hardness of 990 kg/mm^2, which represents about a 40% increase over that of the as-sprayed coating. An important feature is the absence of micron-scale primary α-Al_2O_3 in the final nanocomposite material, which is a reflection of the structural uniformity of the original splat-quenched material.

4. Discussion and Conclusions

The location of the $Al_2O_3/13TiO_2$ composition on the equilibrium phase diagram is indicated in Fig. 6. The presence of the nanocrystalline α-Al_2O_3 phase in the water-quenched powder (Fig. 2) can be interpreted as a consequence of significant undercooling of the melt prior to nucleation of primary α-Al_2O_3 grains followed by dendritic growth of the principal *x*-$Al_2O_3{\cdot}TiO_2$ phase. This being the case, the volume fraction of the much harder α-Al_2O_3 phase may be increased by shifting the composition toward the Al_2O_3-rich side of the phase diagram. It is difficult to predict the composition requirement to realize, say, a 50:50 mixture of the two phases, because of the modification of the phase diagram under supercooling conditions. However, it seems that a starting composition of about $Al_2O_3/7TiO_2$ might serve the purpose. Experiments are underway to check this concept.

The importance of this alloy design approach to coating development is that it should enable us to obtain directly by rapid solidification the desired nanocomposite coating structure, consisting of a controlled volume fraction of hard α-Al_2O_3 nanoparticles dispersed in a softer but tougher *x*-phase matrix. This should be possible even under the splat-quenching conditions characteristic of incremental coating deposition by plasma spraying. Heating of the substrate, for example, would be one way to modify the cooling rates experienced by the liquid droplets when they impinge on the substrate.

Another approach, which we are also examining, is to generate multimodal structures from mixed powder feeds. Of particular interest are coatings composed of micron-scale, hard α-Al_2O_3 particles that are bonded together by the softer but tougher metastable, nanocrystalline $Al_2O_3{\cdot}TiO_2$ phase. To obtain such a coating material, it is anticipated that control of the high-temperature solution kinetics of the differently sized oxide-ceramic particles in the original powder feed will be necessary. Because of the high melting point of pure α-Al_2O_3 phase, relative to the Al_2O_3/TiO_2 eutectic, this appears to be a manageable problem.

Acknowledgments

Support from the Office of Naval Research (Contract Nos. N00014-97-1-0249, N00014-97-1-0844, and N00014-98-3-0005) is gratefully acknowledged.

References

1. S.-C. Liao, W.E. Mayo, and K.D. Pae: *Acta Mater.*, 1997, vol. 45 (10), pp. 4027-40.
2. S.-C. Liao, K.D. Pae, and W.E. Mayo: *Nanostr. Mater.*, 1997, vol. 8 (6), pp. 645-56.
3. S.-C. Liao, Y.-J. Chen, B.H. Kear, and W.E. Mayo: *Nanostr. Mater.*, 1998, vol. 10 (6), pp. 1063-79.
4. S.-C. Liao, K.D. Pae, and W.E. Mayo: *Nanostr. Mater.*, 1995, vol. 5 (3), pp. 319-25.
5. M. Cohen, B.H. Kear, and R. Mehrabian: *Proc. 2nd Int. Conf. on Rapid Solidification Processing*, Reston, VA, Claitor Publishing Division, Baton Rouge, LA, 1980, p. 1.
6. R.-S. Zhou and R.L. Snyder: *Acta Cryst.*, 1991, vol. B47, pp. 617-30.
7. S.M. Lang, C.L. Fillmore, and L.H. Maxwell: *J. Res. Nat. Bur. Standards*, 1952, vol. 48 (4), RP 2316, p. 301.